

Fig. S1. General morphology of the dorsal ridge of juvenile and adult sea lamprey (H and E stain). The dorsal ridge in parasitic juveniles contains only white adipose tissue (W); however, a different structure (B) developed within the core of the white adipose tissue in sexually immature adults, captured during their upstream migration to the spawning ground. In mature adults, this structure replaces white adipose tissue in the dorsal ridge, and displays robust sexual dimorphism. B, brown adipose-like tissue; D, dermis; E, epidermis; F, female; M, male; Mu, muscle; W, white adipose tissue. Scale bars, 500 μ m.

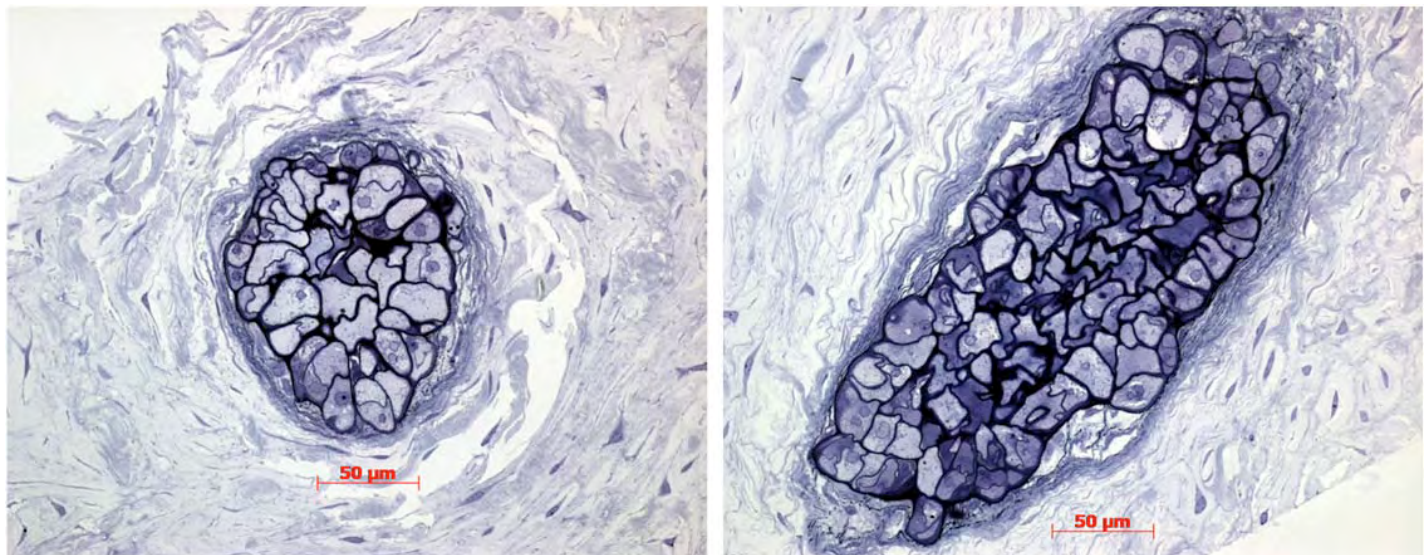


Fig. S2. Toluene-Blue-stained unmyelinated nerve bundles in the rope tissue.

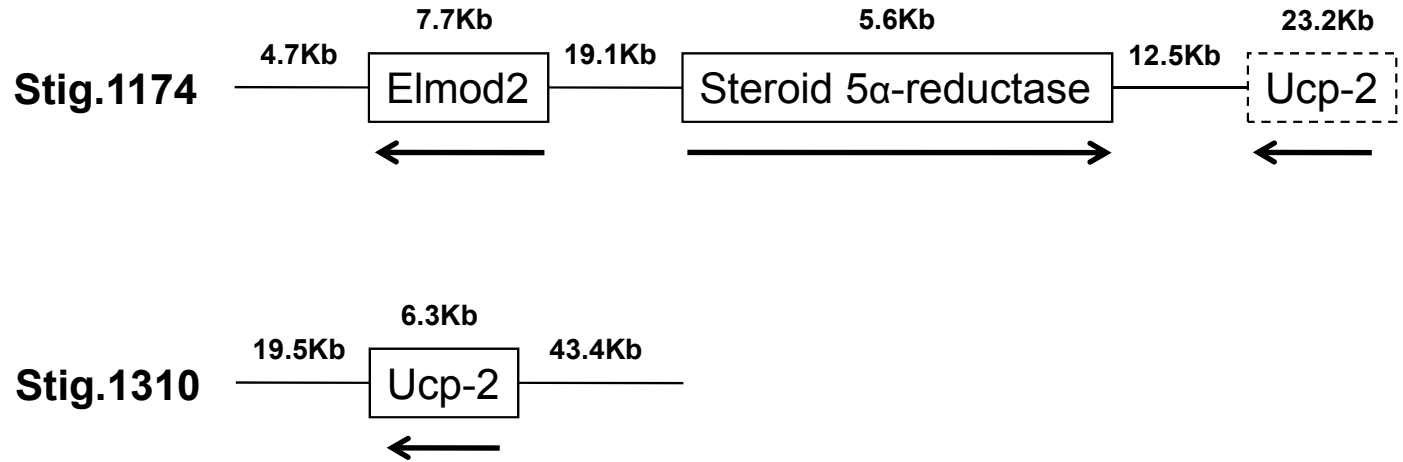


Fig. S3. Gene synteny of *Ucp* genes in sea lamprey genome assembly 2.0 (Libants et al., 2009).

Appendix S1

Additional figure legend for Fig. 12

Fig. 12. (A) X-axis: 1.GO0048856: anatomical structure development, 2.GO0007275: multicellular organismal development, 3.GO0048731: system development, 4.GO0044281: small molecule metabolic process, 5.GO0065008: regulation of biological quality, 6.GO0048869: cellular developmental process, 7.GO0030154: cell differentiation, 8.GO0003008: system process, 9.GO0006629: lipid metabolic process, 10.GO0044255: cellular lipid metabolic process, 11.GO0051239: regulation of multicellular organismal process, 12.GO0022610: biological adhesion, 13.GO0007155: cell adhesion, 14.GO0032879: regulation of localization, 15.GO0006468: protein amino acid phosphorylation, 16.GO0007267: cell-cell signaling, 17.GO0050790: regulation of catalytic activity, 18.GO0065009: regulation of molecular function, 19.GO0044093 positive regulation of molecular function, 20.GO0043085: positive regulation of catalytic activity, 21.GO0051345: positive regulation of hydrolase activity, 22.GO0051336: regulation of hydrolase activity, 23.GO0006928: cellular component movement, 24.GO0016477: cell migration, 25.GO0040011: locomotion, 26.GO0051674: localization of cell, 27.GO0048870: cell motility, 28.GO0007243: protein kinase cascade, 29.GO0010740: positive regulation of protein kinase cascade, 30.GO0010647: positive regulation of cell communication, 31.GO0009967: positive regulation of signal transduction, 32.GO0023056: positive regulation of signaling process, 33.GO0005975: carbohydrate metabolic process, 34.GO0006066: alcohol metabolic process, 35.GO0006952: defense response, 36.GO0007167: enzyme linked receptor protein signaling pathway, 37.GO0007169: transmembrane receptor protein tyrosine kinase signaling pathway, 38.GO0006811: ion transport, 39.GO0006812: cation transport, 40.GO0030001: metal ion transport, 41.GO0040008: regulation of growth, 42.GO0090066: regulation of anatomical structure size, 43.GO0040007: growth, 44.GO0032535: regulation of cellular component size, 45.GO0008361: regulation of cell size, 46.GO0016049: cell growth, 47.GO0006897: endocytosis, 48.GO0010324: membrane invagination, 49.GO0044057: regulation of system process, 50.GO0006936: muscle contraction, 51.GO0003012: muscle system process, 52.GO0007015: actin filament organization, 53.GO0030029: actin filament-based process, 54.GO0030036: actin cytoskeleton organization, 55.GO0009117: nucleotide metabolic process, 56.GO0006753: nucleoside phosphate metabolic process, 57.GO0006164: purine nucleotide biosynthetic process, 58.GO0006163: purine nucleotide metabolic process, 59.GO0048584: positive regulation of response to stimulus, 60.GO0016337: cell-cell adhesion, 61.GO0001501: skeletal system development, 62.GO0051240: positive regulation of multicellular organismal process, 63.GO0032147: activation of protein kinase activity, 64.GO0051347: positive regulation of transferase activity, 65.GO0045860: positive regulation of protein kinase activity, 66.GO0033674: positive regulation of kinase activity, 67.GO0000165: MAPKKK cascade, 68.GO0031098: stress-activated protein kinase signaling pathway, 69.GO0048667: cell morphogenesis involved in neuron differentiation, 70.GO0019318: hexose metabolic process, 71.GO0005996: monosaccharide metabolic process, 72.GO0016052: carbohydrate catabolic process, 73.GO0046365: monosaccharide catabolic process, 74.GO0006007: glucose catabolic process, 75.GO0019320: hexose catabolic process, 76.GO0046164: alcohol catabolic process, 77.GO0044275: cellular carbohydrate catabolic process, 78.GO0030705: cytoskeleton-dependent intracellular transport, 79.GO0008015: blood circulation, 80.GO0003013: circulatory system process, 81.GO0003018: vascular process in circulatory system, 82.GO0035150: regulation of tube size, 83.GO00050880: regulation of blood vessel size, 84.GO0030198: extracellular matrix organization, 85.GO0043062: extracellular structure organization, 86.GO0006643: membrane lipid metabolic process, 87.GO0006665: sphingolipid metabolic process, 88.GO0055085: transmembrane transport, 89.GO0010517: regulation of phospholipase activity, 90.GO0060191: regulation of lipase activity, 91.GO0015674: di-, tri-valent inorganic cation transport, 92.GO0010959: regulation of metal ion transport, 93.GO0043269: regulation of ion transport, 94.GO0022604: regulation of cell morphogenesis, 95.GO0002764: immune response-regulating signaling pathway, 96.GO0002757: immune response-activating signal transduction, 97.GO0002443: leukocyte mediated immunity, 98.GO0002449: lymphocyte mediated immunity, 99.GO0007229: integrin-mediated signaling pathway, 100.GO0006509: membrane protein ectodomain proteolysis, 101.GO0033619: membrane protein proteolysis, 102.GO0045444: fat cell differentiation, 103.GO0019915: lipid storage, 104.GO0007173: epidermal growth factor receptor signaling pathway, 105.GO0019722: calcium-mediated signaling, 106.GO0043410: positive regulation of MAPKK cascade, 107.GO0045744: negative regulation of G-protein coupled receptor protein signaling pathway, 108.GO0043112: receptor metabolic process, 109.GO0031623: receptor internalization, 110.GO0015698: inorganic anion transport, 111.GO0006814: sodium ion transport, 112.GO0009653: anatomical structure morphogenesis, 113.GO0009888: tissue development, 114.GO0048513: organ development, 115.GO0023034: intracellular signaling pathway, 116.GO0007166: cell surface receptor linked signaling pathway, 117.GO0023033: signaling pathway, 118.GO0007154: cell communication, 119.GO0010646: regulation of cell communication, 120.GO0009966: regulation of signal transduction, 121.GO0023051: regulation of signaling process. Y-axis: 1.DRD2, 2.EIF2AK3, 3.NRG1, 4.INSR, 5.BMPR2, 6.TGFB2, 7.TGFBRI, 8.APP, 9.SLIT2, 10.PLCE1, 11.SOD1, 12.ADRB2, 13.MUL1, 14.MAP3K7, 15.TRAF6, 16.PAK1, 17.TPD52L1, 18.RIPK1, 19.TLR6, 20.FKBP1A, 21.PTPRC, 22.NOS1, 23.CHRNB2, 24.RPS27A/UBB, 25.ALDOA, 26.ALDOB, 27.PRKAG2, 28.CDH13, 29.NF2, 30.RELN, 31.TCF7L2, 32.FLNA, 33.NOD2, 34.TLR2, 35.ARRB2, 36.HDAC6, 37.WWC1, 38.ADAM10, 39.ERBB2IP, 40.PPP2CA, 41.PPT1, 42.F2, 43.MYL2, 44.MAPT, 45.SOCS5, 46.AMOT, 47.MYH7, 48.MYL3, 49.TNNC1, 50.LIMK1, 51.ACTA1, 52.ACTC1, 53.PPAP2A, 54.SHC1, 55.DBNL, 56.FPR1, 57.IRAK3,

58.LBP, 59.ATP2A1, 60.ARF6, 61.CNTN4, 62.NLGN1, 63.GRIK2, 64.LGI1, 65.FOXD1, 66.ACVR1, 67.NOG, 68.SOX4, 69.DTX1, 70.PRDM16, 71.FGFR1, 72.FGF12, 73.FGF14, 74.FOXC2, 75.PTN, 76.HSPD1, 77.MSH6, 78.YWHAG, 79.DOCK7, 80.STMN3, 81.DIAP1, 82.DHCR24, 83.GPX3, 84.GRB2, 85.SORT1, 86.FYN, 87.NPR2, 88.CAP2, 89.GRM7, 90.ATP5B, 91.CAP1, 92.KDR, 93.IGFBP5, 94.PDGFR_A, 95.BBS2, 96.JMY, 97.FN1, 98.LYST, 99.SERPINE2, 100.VEGFC, 101.CBLL1, 102.ITGB1BP1, 103.ITGB1, 104.ROCK1, 105.PLG, 106.THBS4, 107.COL5A1, 108.LAMC1, 109.SBDS, 110.NR2F2, 111.PEX13, 112.VCAN, 113.LRP1, 114.EEF1E1, 115.SLC35B2, 116.GOLT1B, 117.SLC20A1, 118.AKAP12, 119.AKAP5, 120.GRB10, 121.GTF2H2, 122.FLT1, 123.GLI3, 124.RGS7, 125.HMGXB4, 126.PFTK1, 127.LPAR1, 128.FGD6, 129.PDCD4, 130.DEPDC6, 131.FICD, 132.RGN, 133.TSC1, 134.BCL2, 135.CHRNA4, 136.SLC30A1, 137.SCN8A, 138.ATP2A2, 139.CACNB2, 140.ARRB1, 141.ARHGEF2, 142.AGPAT9, 143.PIGU, 144.GMIP, 145.RAP1GAP, 146.GPS1, 147.RGS3, 148.PLEKHA1, 149.SLA2, 150.SNX6, 151.SHOC2, 152.HSP90AB1, 153.TAX1BP3, 154.GIT2, 155.GRK6, 156.NLK, 157.PRKCZ, 158.JAK2, 159.SEMA4C, 160.TAO3, 161.MYD88, 162.TNFRSF1A, 163.ATR, 164.GOLPH3, 165.BIRC2, 166.ZDHHC17, 167.TRAF5, 168.TRAF3IP2, 169.RHOC, 170.REL, 171.PLK2, 172.CASP8, 173.LITAF, 174.MTPN, 175.SEMA3A, 176.FGFR1OP, 177.BIN3, 178.PRKCQ, 179.NDRG3, 180.RBBP7, 181.CAMK2D, 182.ATP6V0E, 183.TMEM97, 184.OGFR, 185.NDUFA13, 186.NOL8, 187.EPHX2, 188.GCLM, 189.SOD2, 190.PLA2G10, 191.ABCA1, 192.SOAT1, 193.ITGB3, 194.PPARA, 195.APOB, 196.ITGAV, 197.SERINC1, 198.SERINC5, 199.PDPK1, 200.MRE11A, 201.MAP2K3, 202.STRADA, 203.PSENEN, 204.NCSTN, 205.PSEN2, 206.P2RY4, 207.PLCB2, 208.PPARGC1A, 209.LARGE, 210.ST3GAL6, 211.PYGB, 212.GALK1, 213.NANP, 214.SLC35A3, 215.GAPDHS, 216.GNPDA1, 217.PGD, 218.HK3, 219.PFKP, 220.ACTN4, 221.CALM3, 222.SLC30A5, 223.NEDD4L, 224.CLTC, 225.DNM2, 226.CCND2, 227.P2RY1, 228.NLRP3, 229.STAT1, 230.MSH3, 231.SSBP1, 232.ACE, 233.IGF1R, 234.WNT5A, 235.SDCBP, 236.HMGCR, 237.SMCP, 238.SCYL3, 239.CD2AP, 240.PARP9, 241.PGAM2, 242.RPIA, 243.LDHA, 244.PKM2, 245.SORD, 246.MIOX, 247.TSTA3, 248.FN3K, 249.HISPPD1, 250.PYGL, 251.SLC37A4, 252.DYRK2, 253.UGP2, 254.FBP2, 255.ALDOC, 256.CHST15, 257.CHGA, 258.GCLC, 259.GCSH, 260.PHF17, 261.PAPPA2, 262.ING1, 263.APBB2, 264.HSPA1A, 265.NUBP1, 266.XRN2, 267.NEB, 268.ADD1, 269.KANK1, 270.TAZ, 271.UGCG, 272.BMP1, 273.COL1A1, 274.RACGAP1, 275.ACBSG1, 276.TPP1, 277.LRRC4C, 278.RTN4R, 279.MAL, 280.POU3F1, 281.CLN5, 282.ECE2, 283.DLX5, 284.SNRK, 285.HINFP, 286.CDK5, 287.NTM, 288.CDK5RAP3, 289.NUMB, 290.CLPTM1, 291.HIST1H4A, 292.NOTCH4, 293.DMBT1, 294.UPK1B, 295.UPK1A, 296.SPRR1B, 297.ERCC2, 298.ERCC3, 299.MPV17, 300.WWP1, 301.PAFAH1B3, 302.GSS, 303.SDHA, 304.SPG7, 305.MPPED2, 306.AVIL, 307.BPNT1, 308.EPHB2, 309.GMFB, 310.EXT1, 311.ST8SIA4, 312.FBN1, 313.TEAD4, 314.ANXA2, 315.UFD1L, 316.TRPS1, 317.OSTF1, 318.TLL1, 319.COL18A1, 320.NCL, 321.C1GALT1, 322.HTT, 323.HCK, 324.EDAR, 325.BTD, 326.CASP14, 327.BRCA2, 328.UBE3A, 329.DGCR6, 330.ITGA2, 331.SPOCK1, 332.ADAM22, 333.APBA1, 334.GP1BA, 335.CDH11, 336.CDSN, 337.GPR98, 338.CASQ2, 339.MYL6B, 340.CXCL1, 341.DNM3, 342.SPRY2, 343.BMP3, 344.PMP22, 345.COL5A2, 346.COL12A1, 347.COL4A4, 348.MYH3, 349.PHYH, 350.ZEB2, 351.TMOD2, 352.MSI1, 353.MAB21L2, 354.LSAM, 355.LIG3, 356.HPCAL4, 357.FABP7, 358.DCLK1, 359.CRIM1, 360.AHNAK, 361.ATN1, 362.SPARC, 363.ALX4, 364.PRDX1, 365.TCF12, 366.SPEG, 367.SGCB, 368.MEF2C, 369.DLX2, 370.MEF2A, 371.TLE3, 372.PITX2, 373.PITX3, 374.PLOD1, 375.CENPF, 376.TIE1, 377.TCFAP2A, 378.SVIL, 379.MYLPF, 380.KRT9, 381.KRT17, 382.KRT13, 383.COL7A1, 384.CTGF, 385.BAI1, 386.ATL1, 387.DCC, 388.TUBB3, 389.FEZ2, 390.NRXN3, 391.EIF2B5, 392.JARID2, 393.CIT, 394.TRAPP4, 395.BBS7, 396.SDF4, 397.SMARCA1, 398.TPD52, 399.LDB1, 400.AQP3, 401.HOXA7, 402.ZFHX3, 403.ERC1, 404.MINK1, 405.TLR8, 406.TUBB2C, 407.SYP, 408.ATXN3, 409.AMPH, 410.GAL, 411.SNAP25, 412.SYT1, 413.SLC1A3, 414.RAB14, 415.GRIK5, 416.BSN, 417.GABARAP, 418.BCL3, 419.CARD11, 420.NLRC3, 421.SYNGR3, 422.ADAP1, 423.CSTB, 424.CCNT1, 425.NFKB1, 426.HIP1, 427.ABL2, 428.POR, 429.VCP, 430.CYCS, 431.HSPE1, 432.NPY1R, 433.ATP5A1, 434.REXO2, 435.DCK, 436.CMPK1, 437.COASY, 438.HPRT1, 439.ACLY, 440.ADCY1, 441.ATP5C1, 442.GNAI2, 443.ENPP3, 444.UMPS, 445.PDE8B, 446.ADK, 447.NME6, 448.SLC25A13, 449.AMPD2, 450.ADCY2, 451.ADSL, 452.CHIA, 453.ARNT, 454.POLR3C, 455.MYH4, 456.GAMT, 457.CRYAB, 458.SLC6A8, 459.MYH8, 460.MYH13, 461.KBTBD10, 462.DAG1, 463.DYSF, 464.DES, 465.TPM3, 466.TNNT1, 467.TNNC2, 468.TNNI1, 469.PVR, 470.HPGD, 471.DUOX1, 472.PTPRG, 473.EPS8, 474.GAB1, 475.SLC7A5, 476.ADAM11, 477.PTK2, 478.MAGI1, 479.GP1BB, 480.TNFRSF14, 481.TACSTD2, 482.P2RY5, 483.IL17RA, 484.GPR133, 485.GNB2, 486.CRHR2, 487.BIRC3, 488.BRD8, 489.GABRA2, 490.GUCA1B, 491.SCG5, 492.SLC5A7, 493.ABAT, 494.ALDH9A1, 495.KIF1B, 496.GAD1, 497.SLC6A2, 498.SCN2B, 499.RAPSN, 500.GRIA2, 501.DLGAP2, 502.GLRA3, 503.TNFAIP6, 504.ATG4B, 505.TUSC2, 506.TRHDE, 507.PCDH8, 508.ASH1L, 509.MME, 510.PFN2, 511.RALA, 512.ARPC1A, 513.DOCK2, 514.AIF1, 515.ARPC4, 516.ATP6V1H, 517.CUBN, 518.LRP8, 519.LRP2, 520.VAMP7, 521.TUB, 522.SORL1, 523.RAB5A, 524.RAB7, 525.MCL1, 526.SYNE1, 527.KRT19, 528.DNM1L, 529.IFT172, 530.SIX4, 531.MCAM, 532.IGF2BP2, 533.IGF2BP3, 534.KHDRBS1, 535.FZD1, 536.TACR3, 537.SORCS3, 538.LPHN3, 539.LPHN2, 540.LAMA1, 541.GPR124, 542.BAI3, 543.CPE, 544.SMAD1, 545.RAPGEF1, 546.PXN, 547.PIK3R3, 548.FIBP, 549.FLT4, 550.SLC4A11, 551.SLC12A2, 552.LASP1, 553.SLC13A4, 554.CLIC5, 555.ANO1, 556.CLIC1, 557.CACNA1C, 558.ITPR1, 559.TRPV5, 560.SCN3A, 561.TRAPP4, 562.RHAG, 563.CCS, 564.UCP2, 565.ATP6V0D1, 566.ATP6V1F, 567.MAP4K3, 568.DUSP4, 569.MAPK10, 570.MAP2K7, 571.CRKL, 572.MAP2K4, 573.PTGS1, 574.SDR16C5, 575.OSBPL1A, 576.ACAA2, 577.CELA3B, 578.CHKA, 579.DPAGT1,

580.ACADVL, 581.RETSAT, 582.SC4MOL, 583.PECI, 584.FADS3, 585.FADS2, 586.ELOVL4, 587.ECH1, 588.CPT1B, 589.CPT1A, 590.BDH2, 591.ACOT11, 592.ACSBG2, 593.NANS, 594.PTGIS, 595.MGST3, 596.GPX5, 597.GPR175, 598.GDE1, 599.CPNE7, 600.ACSS2, 601.CPNE3, 602.PRDX6, 603.PLAC8, 604.PIK3C2A, 605.PIGT, 606.PIGF, 607.PI4K2A, 608.PGAP3, 609.CDS2, 610.IP6K1, 611.NAGA, 612.NEU3, 613.SPTLC2, 614.SPTLC1, 615.SMPD2, 616.SGPL1, 617.ASAH1, 618.GM2A, 619.SLC23A1, 620.ATOX1, 621.SGK1, 622.AC CN2, 623.SCN1A, 624.SLC25A12, 625.FXYD1, 626.SLC4A10, 627.SLC22A18, 628.SLC22A3, 629.NFE2L1, 630.EYA4, 631.FZD2, 632.FBN2, 633.EZH1, 634.CST6, 635.CYR61, 636.BBS1, 637.ADAM12, 638.VHL, 639.MPZL2, 640.MUC5AC, 641.FERMT2, 642.ARHGDIA, 643.TGM2, 644.PPFIA2, 645.PLEKHA2, 646.ITGA1, 647.ISLR, 648.HABP2, 649.CIB1, 650.CASK, 651.BYSL, 652.ACTN2, 653.BCAM, 654.CDH1, 655.PVRL3, 656.CLDN19, 657.CLDN9, 658.MAST2, 659.CTBP1, 660.NME5, 661.CUGBP1, 662.ZCCHC11, 663.ANXA13, 664.SRA1, 665.CTBP2, 666.MED1, 667.COL6A2, 668.CD93, 669.PVRL1, 670.TLN2, 671.TGFBI, 672.PPFIBP1, 673.NELL2, 674.MAEA, 675.LRRN2, 676.LGALS4, 677.FBLN5, 678.ACTN3, 679.COL6A1, 680.CLDN6, 681.LGALS7, 682.SMPD4, 683.LASS1, 684.NSMAF, 685.SREBF1, 686.PITPNB, 687.FDXR, 688.FDFT1, 689.FABP6, 690.ABCB4, 691.ACP6, 692.PLCD1, 693.AGPAT3, 694.PIP5K1A, 695.ALDH8A1, 696.RBP1, 697.PTGR1, 698.FASN, 699.PEX7, 700.CHKB, 701.DPM1, 702.RND3, 703.SSH2, 704.PRKG1, 705.CFL1, 706.PLEK2, 707.RAB18, 708.GULP1, 709.CORO1C, 710.ANXA11, 711.AP1S1, 712.STON1, 713.STON2, 714.TIMP3, 715.SH3D19, 716.COL4A6, 717.PXDN, 718.SMARCB1, 719.LRPAP1, 720.CHEK1, 721.RSF1, 722.CTCF, 723.ID2, 724.PIF1, 725.RBL1, 726.MGAM, 727.MGAT4A, 728.GALNT5, 729.B4GALNT1, 730.DDH, 731.HYAL4, 732.CHIT1, 733.FUCA1, 734.LCP1, 735.UNC13D, 736.EHD1, 737.MXI1, 738.TXNRD3, 739.STX12, 740.SHANK1, 741.RFC1, 742.PCSK7, 743.FTH1, 744.CPN2, 745.AGR2, 746.CP, 747.CDO1, 748.SLC7A7, 749.SLC7A6, 750.SDS, 751.PSPH, 752.PON3, 753.PEPD, 754.PCYOX1, 755.NME4, 756.NFS1, 757.MDH2, 758.MARS2, 759.KARS, 760.GGT1, 761.GATAD2A, 762.CBS, 763.CBR1, 764.CARS, 765.ASL, 766.ACO2, 767.AMD1, 768.STT3B, 769.MGAT2, 770.IDUA, 771.IDH3A, 772.GALK2, 773.CNOT7, 774.CS, 775.ALDH2, 776.IDH1, 777.IDH3G, 778.DDX58, 779.NMI, 780.MGLL, 781.UMOD, 782.PRDX5, 783.PLA2G2D, 784.NFRKB, 785.NCF2, 786.MX1, 787.GPR68, 788.CBARA1, 789.F11R, 790.PRKACA, 791.MAP2K6, 792.FASTK, 793.CREB1, 794.EPHA5, 795.SRPK1, 796.DAPK3, 797.MAP4K4, 798.STK36, 799.POFUT1, 800.ZMYM6, 801.PRELID1, 802.BST1, 803.PHF3, 804.PROL1, 805.ASPH, 806.CAMTA2, 807.PITPPNA, 808.U NC13B, 809.TIMM13, 810.TIMM10, 811.SCNN1G, 812.SCNN1A, 813.RABGGTA, 814.OAT, 815.GJA8, 816.KIFC3, 817.TOLLIP, 818.MAP1LC3A, 819.INPP5A, 820.GJD3, 821.ATG3, 822.ATG4C, 823.MLLT4, 824.SH3KBP1, 825.MYO1E, 826.LRP PRC, 827. UXT, 828.CCDC88C, 829.STK39, 830.PIK3R4, 831.MAP3K1, 832.MAK, 833.LIPE, 834.DYRK4, 835.ALK, 836.CDK9, 837.WNK1, 838.PRKCSH, 839.WNK2, 840.SOCS6, 841.CAML, 842.CALCOCO2, 843.ABCF1, 844.AOX1, 845.MAP2K1, 846.WASL, 847.TPM4, 848.DNAL1I, 849.CAPZB, 850.CAPZA2, 851.CAPZA1, 852.ARPC3, 853.ARPC2, 854.ARPC1B, 855.ACTR2, 856.ACTR3, 857.OTOR, 858.SLC26A5, 859.CRYM, 860.U NC84A, 861.UBE2C, 862.TFP1, 863.TERF2, 864.SUPT7L, 865.SMG6, 866.SLC9A7, 867.CREBBP, 868.BUB3, 869.CACNA1A, 870.SLC19A2, 871.GIF, 872.GRPEL1, 873.NEFL, 874.DYNC1II, 875.KIF1A, 876.BRCC3, 877.BRE, 878.DNAJC1, 879.GAPVD1, 880.HELLS, 881.RS1, 882.LIMD1, 883.ARIH2, 884.HOXA5, 885.SLC7A8, 886.CAD, 887.SHMT2, 888.QPRT, 889.PRMT5, 890.PPME1, 891.PDXK, 892.P4HB, 893.MTAP, 894.METTL3, 895.KMO, 896.IVD, 897.IDO2, 898.HPD, 899.GATM, 900.FTCD, 901.DERA, 902.DDO, 903.CXXC1, 904.BCKDK, 905.BCKDHA, 906.AOF1, 907.AADAT, 908.ALDH6A1, 909.VIM, 910.MCTP1, 911.ERCC8, 912.RNF8, 913.GC, 914.PEX5, 915.ATP1A2, 916.RENBP, 917.MYOF, 918.SCN5A, 919.MYL1, 920.MYL7, 921.SEMA6A, 922.STAT3, 923.MYH9, 924.JAG2, 925.LAMA5, 926.CEACAM1, 927.SYK, 928.VEGFA, 929.NOTCH2, 930.ERBB3, 931.NOTCH1, 932.ACVR2A, 933.ACVR2B, 934.KLK14, 935.SALL1, 936.ADAM9, 937.ROBO1, 938.SCRIB, 939.ANGPTL3, 940.EDNRB, 941.NPR1, 942.PLA2G1B, 943.SNCA. (B) X-axis: 1.GO0048856: anatomical structure development, 2.GO0016310: phosphorylation, 3.GO0009653: anatomical structure morphogenesis, 4.GO0006928: cellular component movement, 5.GO0010647: positive regulation of cell communication, 6.GO0051336: regulation of hydrolase activity, 7.GO0006820: anion transport, 8.GO0006091: generation of precursor metabolites and energy, 9.GO0055114: oxidation reduction, 10.GO0006119: oxidative phosphorylation, 11.GO0022900: electron transport chain, 12.GO0022904: respiratory electron transport chain, 13.GO0006120: mitochondrial electron transport NADH to ubiquinone, 14.GO0042773: ATP synthesis coupled electron transport, 15.GO0042775: mitochondrial ATP synthesis coupled electron transport, 16.GO0045333: cellular respiration, 17.GO0015980: energy derivation by oxidation of organic compounds, 18.GO0030029: actin filament-based process, 19.GO0048646: anatomical structure formation involved in morphogenesis, 20.GO0061061: muscle structure development, 21.GO0007517: muscle organ development. Y-axis: 1.SDHA, 2.NDUFS4, 3.NDUFV1, 4.NDUFS8, 5.NDUFS6, 6.NDUFS5, 7.NDUFS3, 8.NDUFS2, 9.NDUFC2, 10.NDUFB9, 11.NDUFB8, 12.NDUFB7, 13.NDUFB6, 14.NDUFB4, 15.NDUFB3, 16.NDUFB10, 17.NDUFAB1, 18.NDUFA8, 19.NDUFA7, 20.NDUFA6, 21.NDUFA5, 22.NDUFA4, 23.NDUFA3, 24.NDUFA2, 25.NDUFA1, 26.NDUFA10, 27.NDUFV2, 28.TAZ, 29.SLC25A12, 30.SLC25A13, 31.NF1, 32.MYH7, 33.MYL2, 34.ACTA1, 35.ACTC1, 36.TNNC1, 37.MYL3, 38.NOG, 39.SEMA4C, 40.NRG1, 41.UTRN, 42.TEAD4, 43.SPEG, 44.SGCB, 45.MEF2C, 46.MEF2A, 47.CHRNA1, 48.CACNB2, 49.CAPN3, 50.MYL6B, 51.NEB, 52.CDKN2A, 53.MUL1, 54.SMAD4, 55.SOD1, 56.SLIT2, 57.THBS4, 58.SALL1, 59.CDH13, 60.VEGFA, 61.KCNH1, 62.NOS1, 63.ATP5B, 64.PLG, 65.AAMP, 66.LAMA5,

67.SERPINF1, 68.AGGF1, 69.C1GALT1, 70.ATP5C1, 71.ATP5O, 72.UQCRC2, 73.UQCRB, 74.UQCRH,
 75.RPS27A/UBB, 76.FKBP1A, 77.TGFB2, 78.KRT19, 79.ROBO1, 80.DRD2, 81.SCRIB, 82.PAFAH1B1,
 83.AMOT, 84.MYH9, 85.ADAM12, 86.RHOB, 87.NPR1, 88.CASC5, 89.CTNNB1, 90.SRF, 91.ADAM9,
 92.CEACAM1, 93.CD9, 94.ANXA3, 95.BBS2, 96.RAC1, 97.THBS1, 98.SYK, 99.JAK2, 100.BMPR2,
 101.RELN, 102.TGFBR1, 103.NF2, 104.PLA2G1B, 105.IGFBP3, 106.SIRT2, 107.NOTCH1, 108.MYL6,
 109.MRAS, 110.MYH3, 111.HINFP, 112.ZFHX3, 113.TCF12, 114.MYLPF, 115.MTPN, 116.LMNA,
 117.LAMA2, 118.CENPF, 119.HDAC1, 120.FDXR, 121.SCO2, 122.PXDN, 123.POR, 124.PGD,
 125.PDIA5, 126.DDO, 127.COX15, 128.BLVRA, 129.CDO1, 130.DUOX1, 131.PLOD1, 132.BRSK1,
 133.DOCK7, 134.CDC42, 135.VHL, 136.TLE3, 137.STXBP1, 138.SPRY2, 139.SHROOM3, 140.RTN4R,
 141.NDC80, 142.MAPT, 143.GLI3, 144.FZD2, 145.FBN2, 146.FAT1, 147.EZH1, 148.DNM1L,
 149.DLX5, 150.DIAP1, 151.DCC, 152.CYR61, 153.CYFIP1, 154.CST6, 155.COL5A2, 156.COL1A2,
 157.COL18A1, 158.CAP1, 159.BBS7, 160.ATL1, 161.BBS5, 162.UNC5C, 163.PLA2G10, 164.NRXN3,
 165.LAMC1, 166.FN1, 167.FEZ2, 168.COL5A1, 169.BAMBI, 170.CNTN4, 171.ATM, 172.YWHAG,
 173.GMFB, 174.EPHB2, 175.FGFR1, 176.UGCG, 177.TLL1, 178.TCFAP2A, 179.TAGLN3, 180.STS,
 181.STMN2, 182.ST8SIA4, 183.SPRR1A, 184.SPARC, 185.SMPD1, 186.SH3GL3, 187.SH3GL1,
 188.SDF4, 189.SCNA8, 190.RRM2, 191.RPS14, 192.RBM45, 193.PTN, 194.PRDX1, 195.PPT1,
 196.PMP22, 197.PLK4, 198.PAFAH1B3, 199.OSTF1, 200.NLGN1, 201.NCKAP1, 202.MSI1, 203.MAL,
 204.MAB21L2, 205.LSAMP, 206.LIG4, 207.LIG3, 208.LDB1, 209.KRT9, 210.KRT17, 211.KRT13,
 212.JARID2, 213.HPCAL4, 214.HOXA7, 215.HES1, 216.HCK, 217.GSS, 218.FBN1, 219.EXT1,
 220.ECE2, 221.DTX1, 222.DSP, 223.DNM3, 224.DLX2, 225.DCLK1, 226.CTGF, 227.CRIM1,
 228.COL7A1, 229.COL4A4, 230.CLN5, 231.CIT, 232.CDH11, 233.CASP14, 234.CALR, 235.BPNT1,
 236.BMP3, 237.AVIL, 238.ATN1, 239.AQP3, 240.ANXA2, 241.ALX4, 242.ADAM22, 243.ALPL,
 244.ARHGAP26, 245.CXCL1, 246.NR2F2, 247.VCAN, 248.SBDS, 249.RPS19, 250.ETS1, 251.HMGCR,
 252.F2, 253EIF2AK3, 254.PLCE1, 255.LPAR1, 256.SSBP1, 257.RPS3, 258.RGN, 259.MSH3, 260.LRP1,
 261.HSPE1, 262.HIP1, 263.GNAQ, 264.FICD, 265.BIRC5, 266.CSTB, 267.DHCR24, 268.HSPD1,
 269.TRP63, 270.TRAF3IP2, 271.TMEM101, 272.SLC35B2, 273.RHOC, 274.REL, 275.PLK2, 276.NOD2,
 277.MYD88, 278.LBP, 279.GRIK2, 280.GOLT1B, 281.GOLPH3, 282.EEF1E1, 283.ECT2, 284.AKAP5,
 285.CC2D1A, 286.WWC1, 287.HDAC6, 288.ARRB2, 289.HDAC2, 290.TCF7L2, 291.RHOA,
 292.NOTCH2, 293.SOX4, 294.ERBB3, 295.LGI1, 296.TLR6, 297.TLR2, 298.TAOK3, 299.RIPK1,
 300.MAP3K7, 301.MIF, 302.WNK2, 303.WNK1, 304.VRK1, 305.TRIB2, 306.TPX2, 307.STK17B,
 308.SNX6, 309.RAD17, 310.PPP2CA, 311.PIP5K1A, 312.PIK3R4, 313.PBK, 314.PAK2, 315.PAK1,
 316.MRE11A, 317.MOBKL1A, 318.MCM7, 319.MAST2, 320.MAP3K1, 321.MAP2K6, 322.MAP2K3,
 323.MAK, 324.IP6K1, 325.HEXIM1, 326.GOLGA5, 327.EPHA5, 328.DBNL, 329.DAPK1, 330.CXCR4,
 331.CTBP1, 332.CHEK1, 333.CDK9, 334.CDK2AP1, 335.CD81, 336.CCNE2, 337.CCND2,
 338.CCDC88C, 339.CAD, 340.ABL2, 341.AKTIP, 342.PPAP2A, 343.PDGFR, 344.ADAM10,
 345.FPR1, 346.SLC25A22, 347.SLC25A1, 348.SLC17A5, 349.SLC12A2, 350.FXYD1, 351.ENPP3,
 352.CLIC5, 353.ANO1, 354.CLIC1, 355.VIL1, 356.SSH2, 357.RND3, 358.PRKG1, 359.PLEK2,
 360.PFN2, 361.MYO1E, 362.MYH10, 363.KANK1, 364.GSN, 365.DOCK2, 366.CRK, 367.CFL1,
 368.ARPC4, 369.ADD1, 370.AIF1, 371.VIM, 372.VEGFC, 373.SORD, 374.SERPINE2, 375.SCYL3,
 376.PARP9, 377.LYST, 378.ITGB1, 379.IGFBP5, 380.CUZD1, 381.CBLL1, 382.ARPC3, 383.ARPC2,
 384.ARPC1B, 385.ARHGDIA, 386.ACTR3, 387.ACTR2, 388.ACTN4, 389.ACTB, 390.ACTG1,
 391.SDCBP, 392.AR6, 393.ELMO1, 394.PRDM16, 395.PRKAG2, 396.HK3, 397.GAPDH, 398.ACOX1,
 399.FDX1, 400.AKT2, 401.GFPT1, 402.GAPDHS, 403.ALDOB, 404.UQCR, 405.SLC25A4, 406.PKM2,
 407.PHKB, 408.PHKA1, 409.PFKP, 410.OGDH, 411.FECH, 412.ECH1, 413.CROT, 414.COX7C,
 415.COX7A1, 416.COX6C, 417.COX6A1, 418.COX17, 419.COX4I1, 420.GRB10, 421.NNT, 422.CYCS,
 423.PYGM, 424.PYGB, 425.ACADVL, 426.CRAT, 427.SDHD, 428.SDHB, 429.PPARGC1A, 430.ACO2,
 431.PDHB, 432.SORT1, 433.TSC1, 434.STMN3, 435.VCP, 436.SNCA, 437.RAP1GAP, 438.RALBP1,
 439.PLCB2, 440.P2RY4, 441.P2RY1, 442.GMIP, 443.DIABLO, 444.GABARPL2, 445.LIMK1,
 446.PDPK1, 447.SNRK, 448.DYRK1A, 449.ACVR1, 450.CDK5RAP3, 451.ACVR2A,, 452.TRAF2,
 453.ADRB2, 454.TPD52L1, 455.UGP2, 456.TOLLIP, 457.TNKS, 458.TLK2, 459.STK36, 460.STK11,
 461.SRPK2, 462.SRPK1, 463.SHC1, 464.RGS3, 465.PRKCQ, 466.PGK1, 467.NLK, 468.MINK1,
 469.MAP4K5, 470.LIPE, 471.ITLN1, 472.GPS2, 473.GPS1, 474.FYN, 475.FASTK, 476.DEPDC6,
 477.DAPK3, 478.CDC37, 479.CCNT1, 480.CAMK2G, 481.CAMK2D, 482.ALK, 483.BCKDK,
 484.FLNA, 485.RICTOR, 486.MYL7, 487.LIMA1, 488.MYH4, 489.F10, 490.ACVR2B, 491.UBE2V1,
 492.UBE2N, 493.TNFRSF1A, 494.SLC44A2, 495.LITAF, 496.FLT1, 497.AKAP12, 498.BIRC2,
 499.APC, 500.TPM4, 501.TPM3, 502.SMCP, 503.MAPK14, 504.MAP2K1, 505.AIMP1, 506.DNAL11,
 507.UQCRFS1, 508.COX6B1, 509.ACADL, 510.ACADM, 511.SLC4A11, 512.SLC4A10, 513.SLC1A3,
 514.SLC1A2, 515.GLRA1, 516.SLC13A4, 517.RACGAP1, 518.ACE, 519.ZBTB16, 520.UFD1L,
 521.UBE3A, 522.TRPS1, 523.TRAPP4, 524.TPP1, 525.TMOD2, 526.SNTG2, 527.PHYH, 528.NUMBL,
 529.NPTN, 530.NELL1, 531.NEFH, 532.MPPED2, 533.HIST1H4A, 534.GPR98, 535.GLRX5, 536.FLT3,
 537.FGF14, 538.FGF12, 539.ERCC3, 540EIF2B4, 541EIF2B2, 542EIF2B1, 543.EDAR, 544.DSPP,
 545.DMBT1, 546.DCTN1, 547.CRMP1, 548.COL12A1, 549.CDK5, 550.CASQ2, 551.BTD, 552.BRCA2,
 553.BLOC1S3, 554.ATP2A2, 555.APBA1, 556.ACSEBG1, 557.AGPAT6, 558.WNT5A, 559.TUBB3,
 560.STAT3, 561.SEMA6A, 562.KDR, 563.SEMA3A, 564.TTLL3, 565.SIX4, 566.PITX3, 567.PITX2,
 568.NFE2L1, 569.MCAM, 570.LRRC4C, 571.IGF2BP3, 572.IGF2BP2, 573.IFT172, 574.EYA4,
 575.DGCR6, 576.DGCR2, 577.COL1A1, 578.CLASP2, 579.CLASP1, 580.CAP2, 581.BRAF, 582.BMP1,
 583.ANK1, 584.BAI1, 585.FOXD1, 586.KLK14, 587.FGD6, 588.ALDOA, 589.BIN3.

Sea lamprey rope tissue developmental markers for real-time quantitative PCR

For each marker, the following information is shown: marker name (bold) and NCBI accession number, synthetic oligo used as the standard for real-time quantitative PCR. Yellow blocks show the primer sequences (note: the reverse primer is complementary to the shown sequence). Blue block shows the sequence for TaqMan MGB probe.

PRDM16: PMZ_0000429-RA

cgaccgctcggtcagcatctgtccaaacctgcaggcacgtgcgcaacatccacaacaaggagaagc

Necdin: PMZ_0014623-RA

ggcgcgacgcgatctgacaccgaatttggctccgcacctcggaaatlgcgtttggccgc

PPAR γ : PMZ_0011032-RA

tcacggagttcgccaagtgcataccgggttctggcgtcaacctaatgaccaggtaggggttagtgctgacgctcgat

PGC1 α : PMZ_0014023-RA

gaacgcgtcgcaagtgaaggcgtaagtacaaaaccgttagtgtccctgcggaaacatt

C/EBP γ : PMZ_0021156-RA

cctcggtgtccagaaacagctccttgagcaccacgagctcctggacagcgctggatcttg

UCP: PMZ_0004088-RA

agcgccgttgtttagaagtcttgacggaatcgtagaggccgtgcggaccgaggcgaagctcatctgacgctgcaggc

Heat Generation Calculations for Lamprey Rope Tissue

M. Cody Priess, Yu-Wen Chung-Davidson, Jongeun Choi

November 11, 2011

Heat Transfer Model

The analysis of heat generation in lamprey tissue begins with identification of a correct model. Since the anaesthetised lamprey lies reasonably still in water which is close to its body temperature, the primary method of heat transfer will be free convection. We make the following assumptions about the lamprey and experimental setup in order to make the analysis tractable:

1. The lamprey rope and body are assumed to be perfect cylinders with length much greater than their respective diameters.
2. The heat transfer between the rope tissue and body is assumed to be negligible.
3. Both the mechanical and heat-generating properties of the tissue in the rope and body are assumed to be homogeneous throughout their respective volumes.

We can then model the rope and muscle tissue as long cylinders with uniform volumetric heat generation values Q_{rope} and Q_{muscle} which are losing heat to the water via free convection. When measuring temperature in the rope tissue, the temperature T_{probe} is assumed to be measured by the probe from the geometric center (radially) of the rope. When measuring temperature in the muscle tissue, the measured temperature T_{probe} is assumed to be measured by the probe at a radial distance r from the center of the body. A diagram illustrating this simplified model is shown in Figure 1.

With an approximate knowledge of the water conditions surrounding the lamprey, we can generate a mean convective coefficient \bar{h} which we assume is present over the entire rope surface. This allows us to formulate the heat generation in the rope tissue as a function of the water temperature and the rope temperature. Once the average heat convection coefficient has been determined, we can use the standard temperature equations for a cylindrical body with uniform heat generation and a convective boundary condition [1] in order to relate the probe temperature to the heat generation Q_{rope} .

The mechanical properties of water at $14^{\circ}C$ are listed in Table 1. The thermal conductivity of lamprey tissue k_f is estimated from data in [2] to be

$$k_f \approx 0.5 \text{ W/m} * \text{K}$$

Heat Transfer Analysis

The average convective heat transfer coefficient \bar{h} for a long horizontal cylinder in free convection can be found via the relationship

$$\bar{h} = \frac{k_w}{D} \bar{N}_{u_D} \quad (1)$$

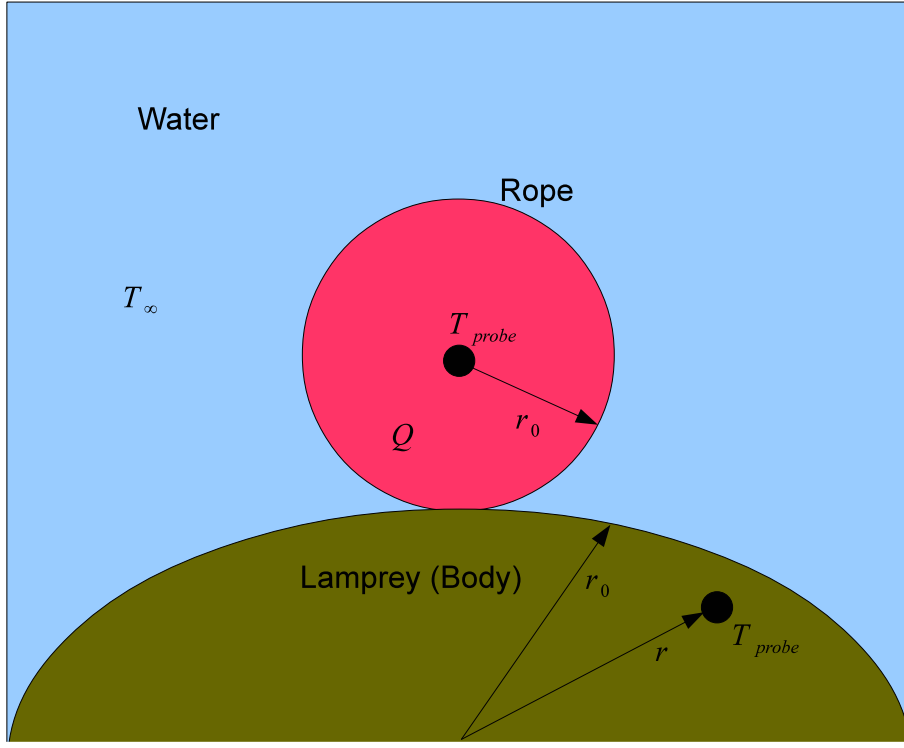


Figure 1: The simplified heat model of the lamprey muscle and rope tissue

| Parameter | Value | Units |
|-----------|------------------------|-----------------|
| ρ | 1000 | kg/m^3 |
| ν | 1.2×10^{-6} | m^2/s |
| c_p | 4.086×10^3 | $J/kg \times K$ |
| k_w | 0.592 | $W/m \times K$ |
| Pr | 8.28 | |
| α | 1.449×10^{-7} | m^2/s |
| β | 114.1×10^{-6} | |
| g | 9.81 | m/s^2 |

Table 1: Physical Properties of water at $\approx 14^\circ C$

where D is the diameter of the cylinder and \bar{N}_{u_D} is the average Nusselt number over the cylinder. There are several methods for finding \bar{N}_{u_D} , but one which is applicable over a wide range of Rayleigh numbers [1] is

$$\bar{N}_{u_D} = \left\{ 0.60 + \frac{0.387 R_{a_D}^{1/6}}{[1 + (0.559/Pr)^{9/16}]^{8/27}} \right\}^2, \quad (2)$$

where the Rayleigh number R_{a_D} is

$$R_{a_D} = \frac{g\beta(T_s - T_\infty)D^3}{\nu\alpha}, \quad (3)$$

and T_s and T_∞ are the temperatures at the surface of the cylinder and the temperature of the water, respectively.

Heat Generation in Rope Tissue

The volumetric heat generation Q of a solid cylinder with convective boundary conditions and internal thermal conductivity k_f with temperature T_{probe} measured at its radial center can be found by solving

$$T_{probe} = \frac{Qr_0^2}{4k_f} + T_s, \quad (4)$$

where r_0 is the radius of the cylinder. Since there is no direct measurement available of the surface temperature T_s , it must be estimated by applying a surface energy balance to the outside of the cylinder, such that

$$\frac{Qr_0}{2} = \bar{h}(T_s - T_\infty). \quad (5)$$

Given (1)-(3), there is no analytical solution to the system of equations defined in (4) and (5), so it must be solved numerically. This was done for each measured temperature value ($T_{probe} - T_\infty$) by using the nonlinear function solver *fsolve* in MATLAB.

Heat Generation in Muscle Tissue

It was desired to compare the heat generation in lamprey muscle tissue to that of the rope tissue in order to determine if the heat generated was simply a function of normal metabolic processes. The heat generation in lamprey muscle tissue was analyzed using a similar procedure to that used for the rope tissue. We again use the relations governing convective heat transfer from a long cylinder, but we no longer assume that the temperature probe is being implanted at the center of the cylinder. We re-write (4) as

$$T_{probe} = \frac{Qr_0^2}{4k_f} \left(1 - \frac{r^2}{r_0^2} \right) + T_s, \quad (6)$$

where r is the distance from the center of the body to the location of probe implantation (measured radially), and r_0 is the diameter of the lamprey body. From here the analysis proceeds identically to that for the rope tissue.

| Lamprey | Rope Mean W/cm^3 | Std. Deviation (W/cm^3) |
|---------|-----------------------|-----------------------------|
| 1 | 2.27×10^{-3} | 6.71×10^{-4} |
| 2 | 7.27×10^{-3} | 4.00×10^{-3} |
| 3 | 4.17×10^{-4} | 3.81×10^{-4} |
| 4 | 1.40×10^{-3} | 5.84×10^{-4} |
| 5 | 1.54×10^{-3} | 1.80×10^{-3} |
| 6 | 3.93×10^{-4} | 4.30×10^{-4} |
| 7 | 1.22×10^{-3} | 5.55×10^{-4} |
| 8 | 2.79×10^{-4} | 3.47×10^{-4} |
| 9 | 6.94×10^{-4} | 2.56×10^{-4} |
| 10 | 7.92×10^{-4} | 3.18×10^{-4} |
| 11 | 8.00×10^{-4} | 3.09×10^{-4} |
| 12 | 1.63×10^{-3} | 4.18×10^{-4} |

Table 2: Mean and standard deviation of Q_{rope} in the 12 tested lamprey

| Lamprey | Muscle Mean W/cm^3 | Std. Deviation (W/cm^3) |
|---------|-----------------------|-----------------------------|
| 1 | 5.32×10^{-5} | 6.32×10^{-5} |
| 2 | 2.39×10^{-4} | 3.78×10^{-5} |
| 3 | 3.61×10^{-5} | 5.55×10^{-5} |
| 4 | 3.84×10^{-5} | 4.52×10^{-5} |
| 5 | 1.56×10^{-4} | 1.76×10^{-4} |
| 6 | 2.88×10^{-5} | 4.43×10^{-5} |
| 7 | 7.68×10^{-6} | 2.44×10^{-5} |
| 8 | 7.93×10^{-5} | 4.44×10^{-5} |
| 9 | 1.46×10^{-5} | 2.15×10^{-5} |
| 10 | 7.33×10^{-5} | 3.54×10^{-5} |
| 11 | 1.25×10^{-4} | 3.76×10^{-5} |
| 12 | 8.28×10^{-5} | 3.72×10^{-5} |

Table 3: Mean and standard deviation of Q_{muscle} in the 12 tested lamprey

Results

Results of the analysis are shown in Figures 2-13. Values used were $D_{rope} = 7.8\text{ mm}$, $D_{body} = 40\text{ mm}$, and $r_{probe} = 16.2\text{ mm}$. The mean and standard deviation of the heat generation in the rope and muscle tissue are shown in Tables 2 and 3, and the ratio of the average heat generation values $Q_{rope,avg}/Q_{muscle,avg}$ for each lamprey is shown in Table 4.

| Lamprey | Ratio Q_{rope}/Q_{muscle} |
|---------|-----------------------------|
| 1 | 42.9 |
| 2 | 30.4 |
| 3 | 11.6 |
| 4 | 36.5 |
| 5 | 9.86 |
| 6 | 13.7 |
| 7 | 159 |
| 8 | 3.52 |
| 9 | 47.5 |
| 10 | 10.8 |
| 11 | 6.41 |
| 12 | 19.7 |

Table 4: Ratio of the average heat generation $Q_{rope,avg}/Q_{muscle,avg}$ for the 12 tested lamprey

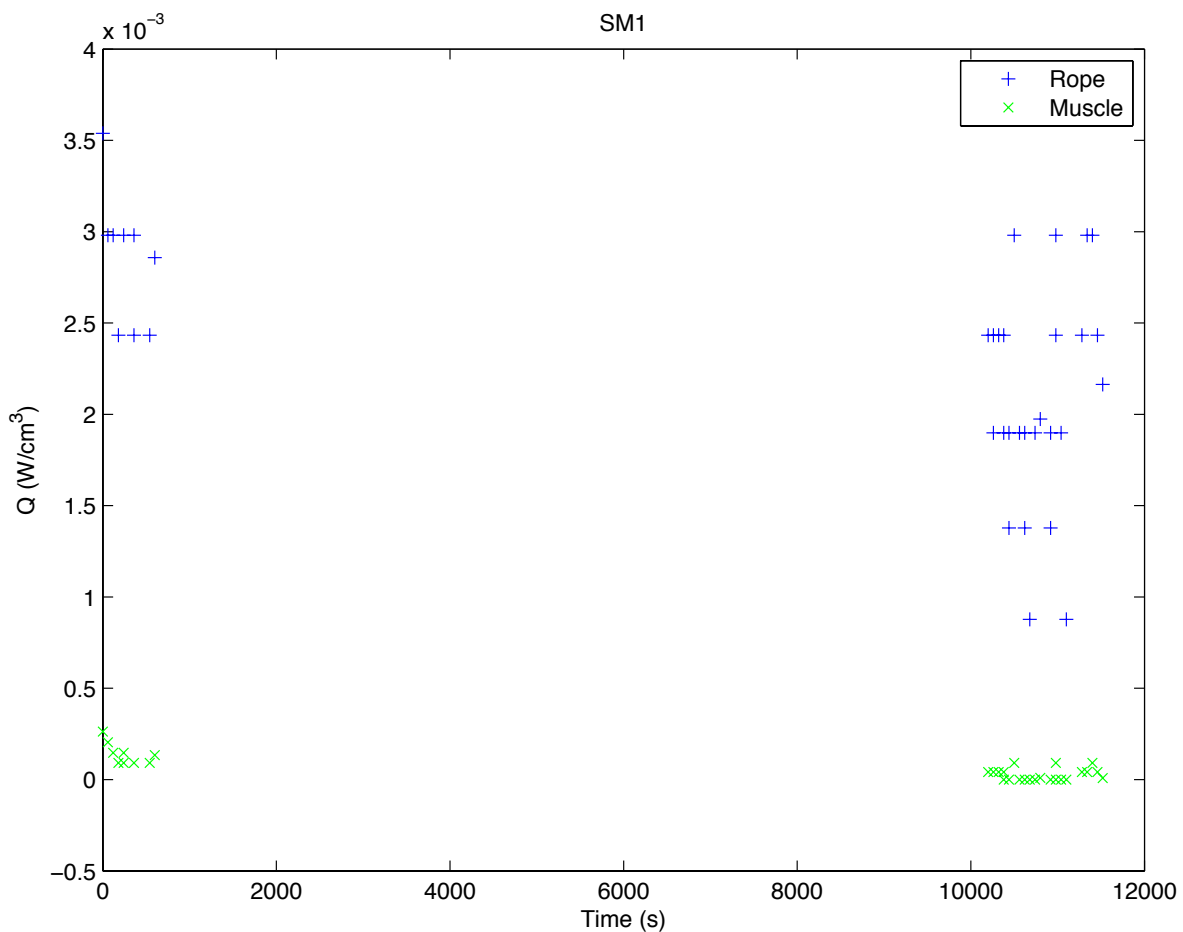


Figure 2: Heat generation in Lamprey 1

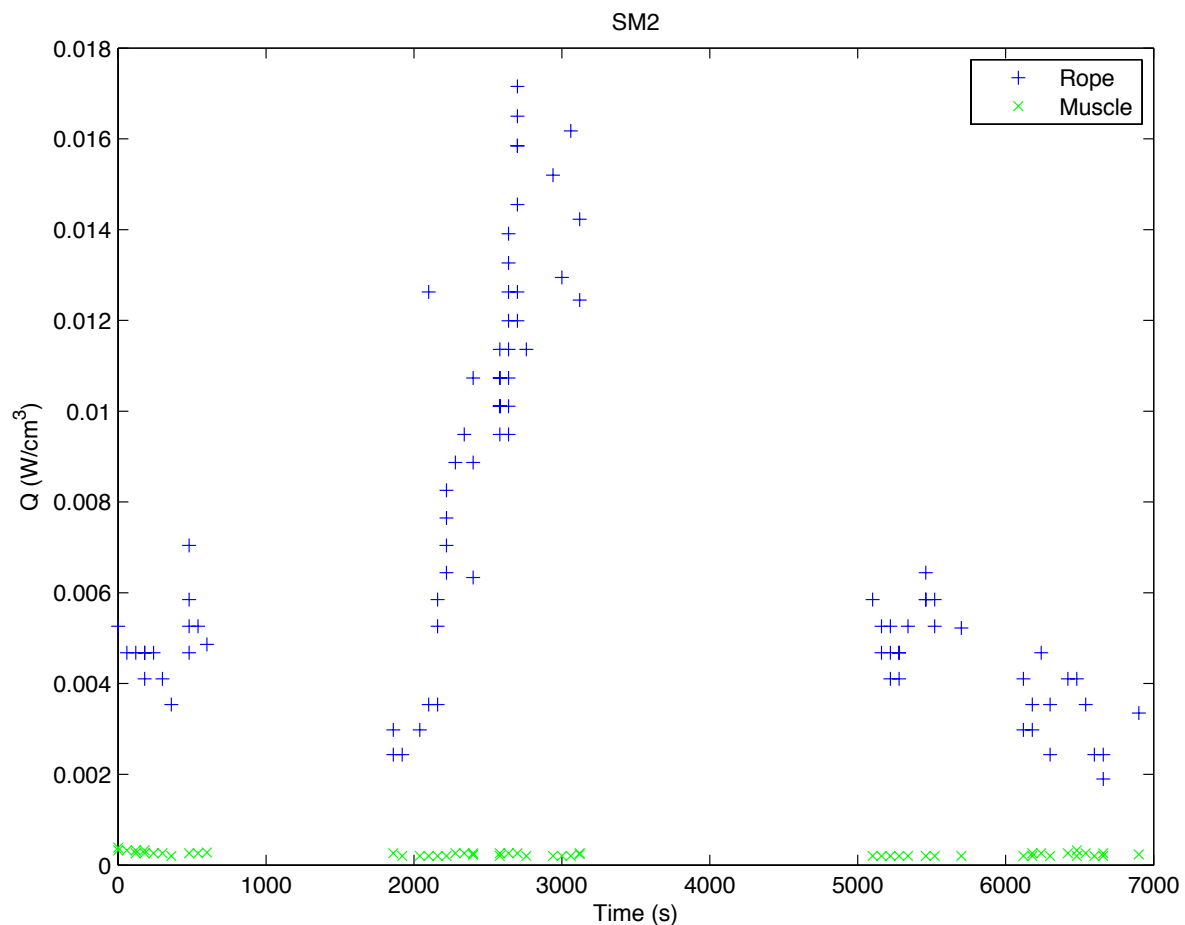


Figure 3: Heat generation in Lamprey 2

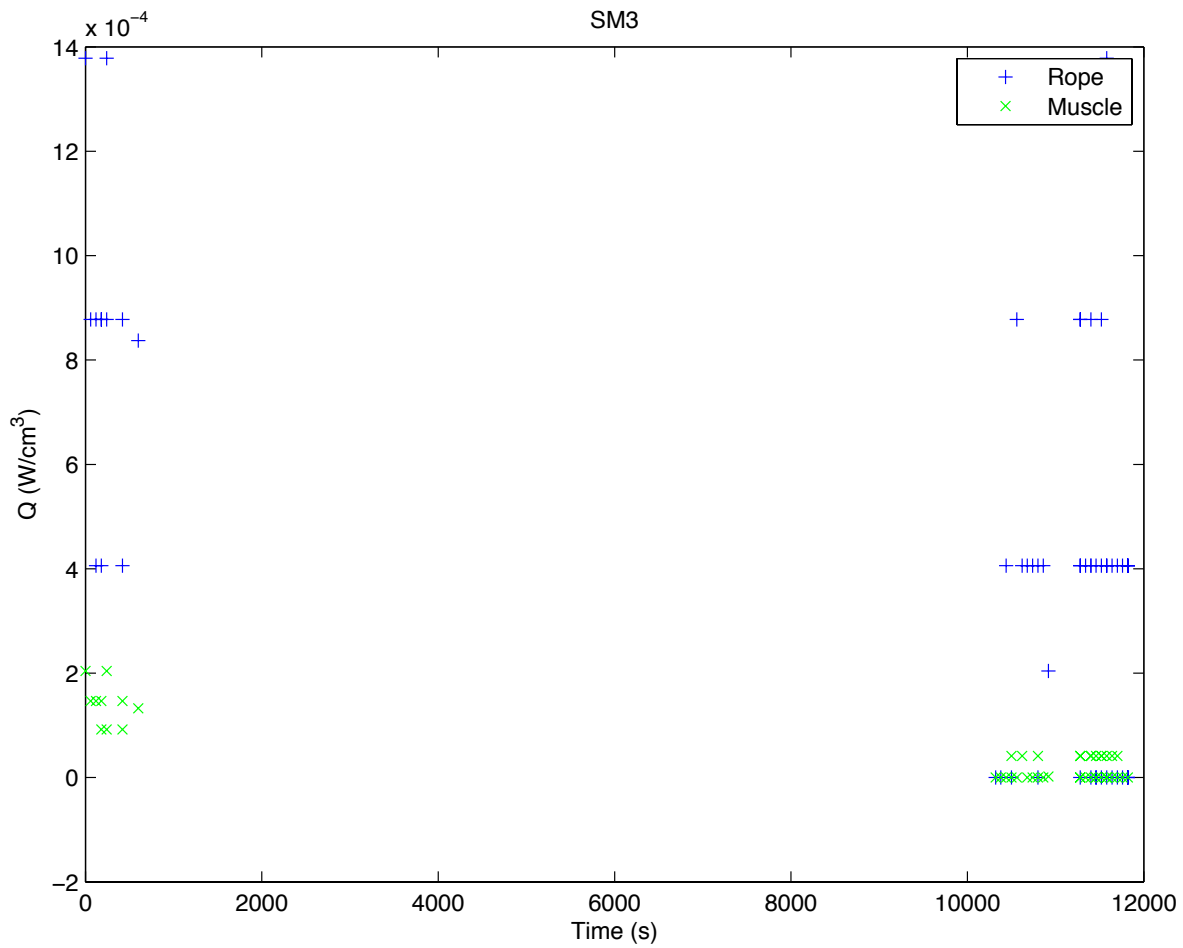


Figure 4: Heat generation in Lamprey 3

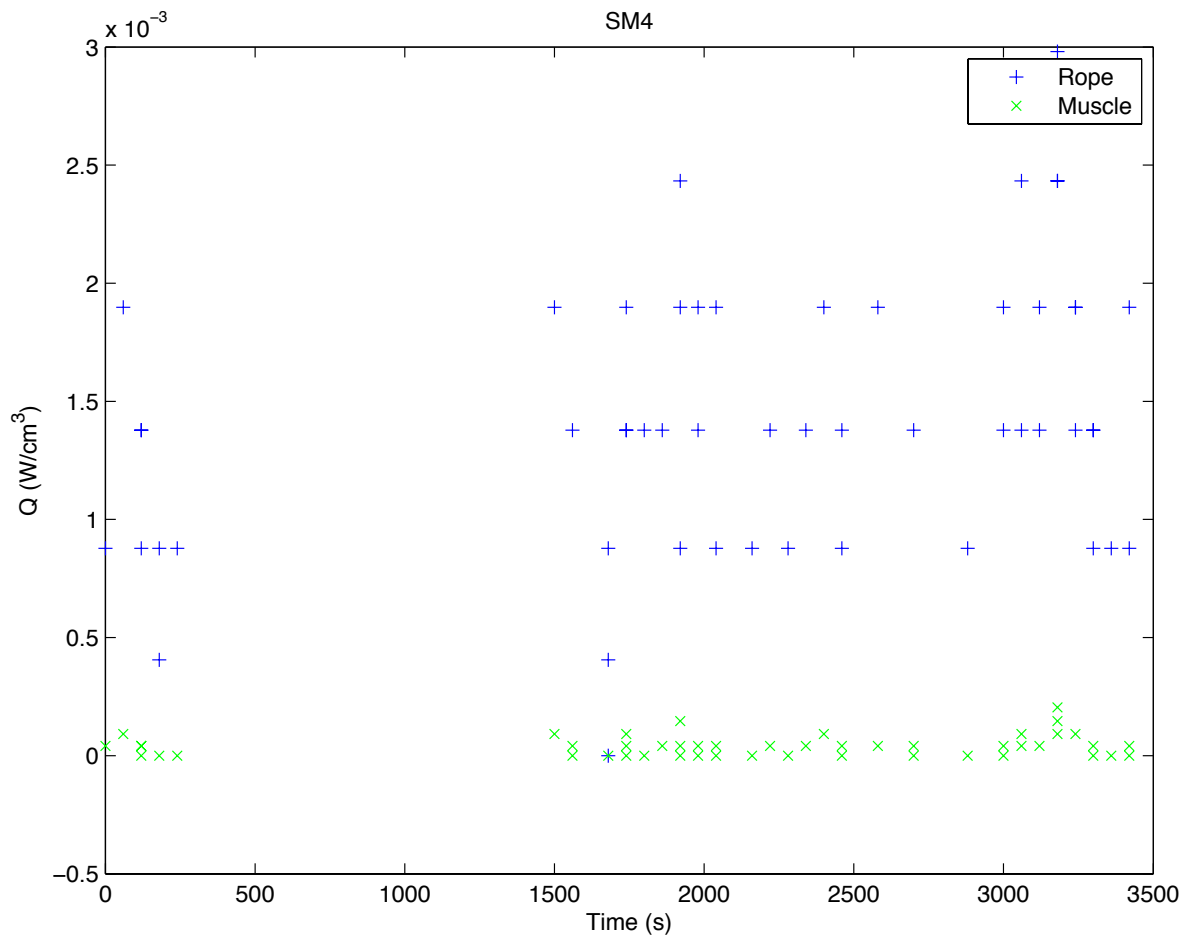


Figure 5: Heat generation in Lamprey 4

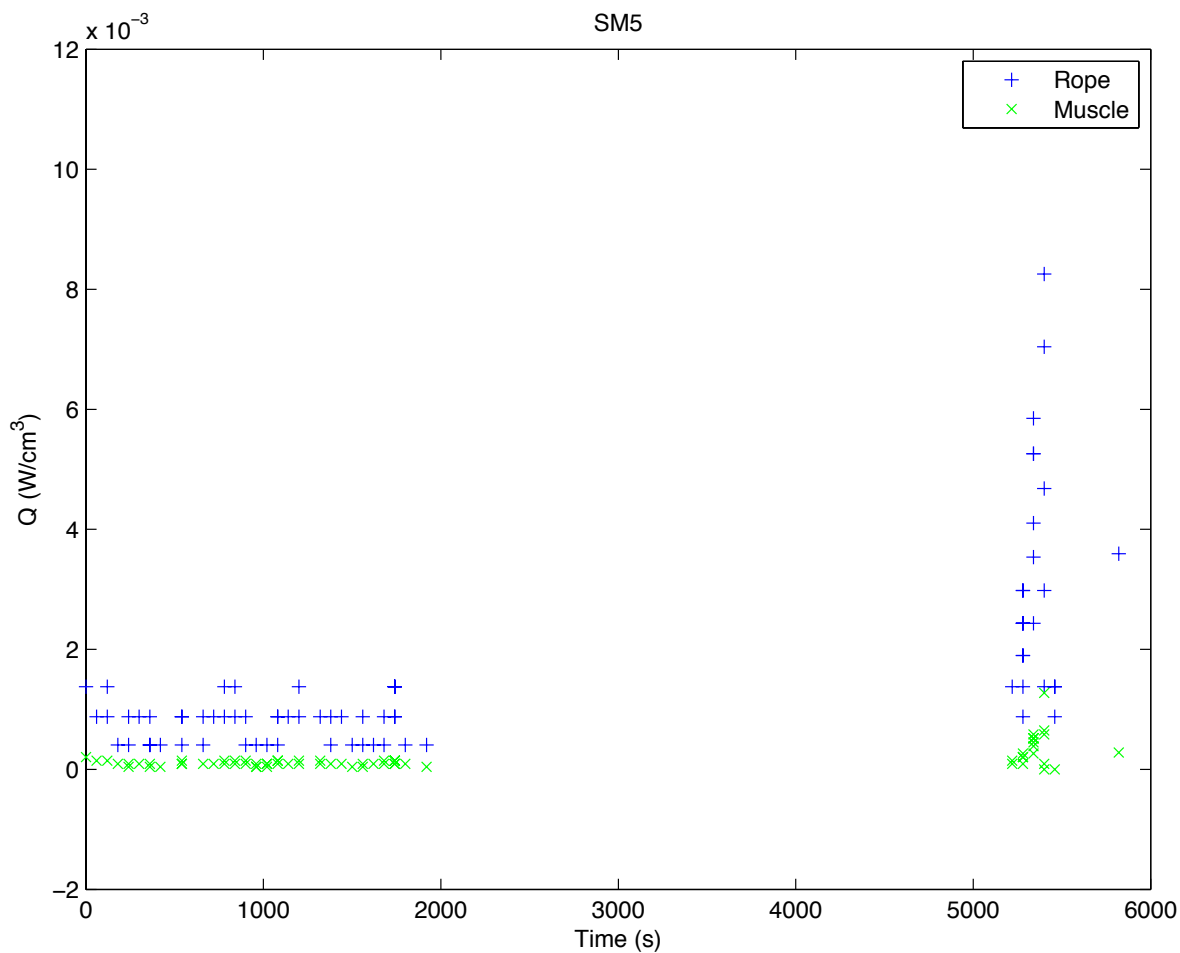


Figure 6: Heat generation in Lamprey 5

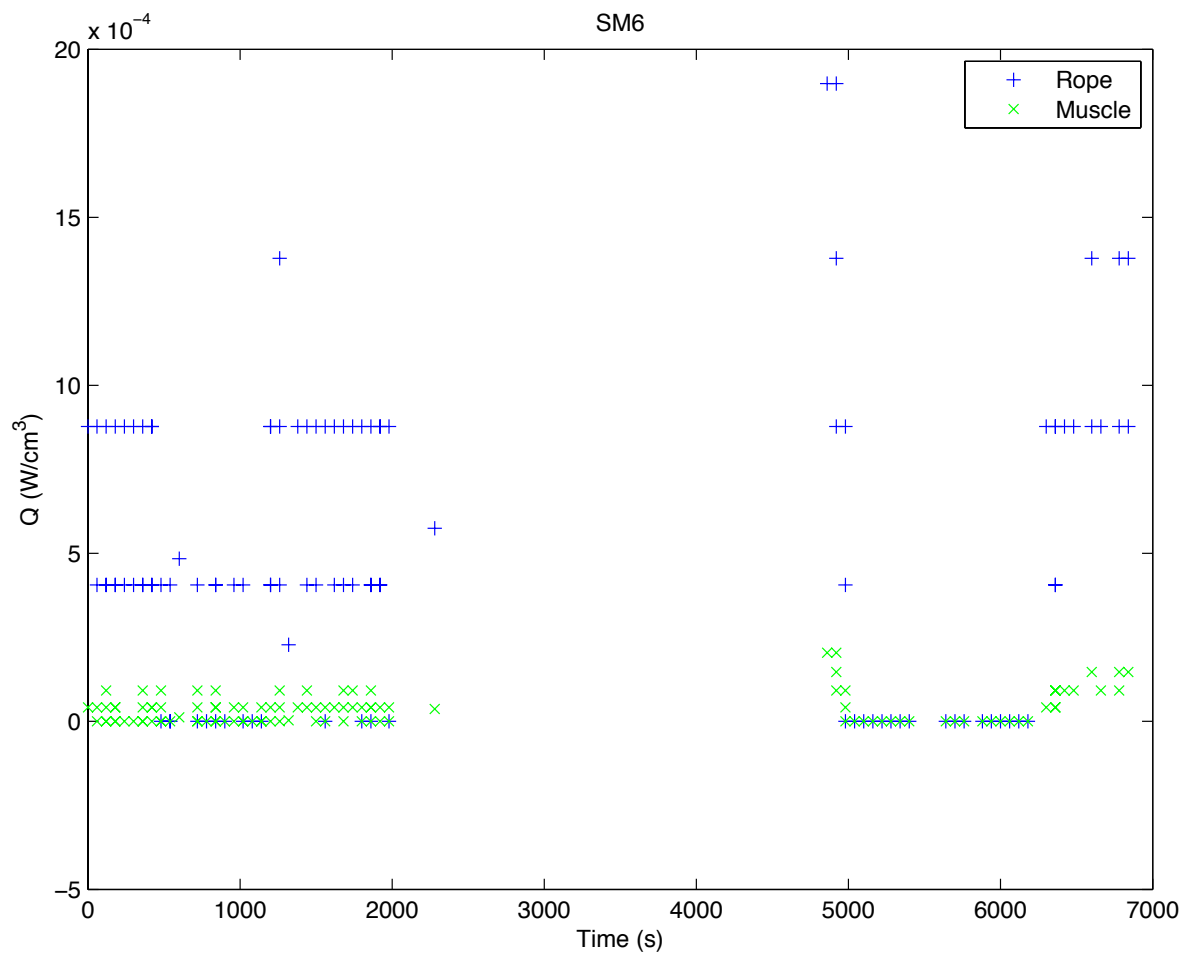


Figure 7: Heat generation in Lamprey 6

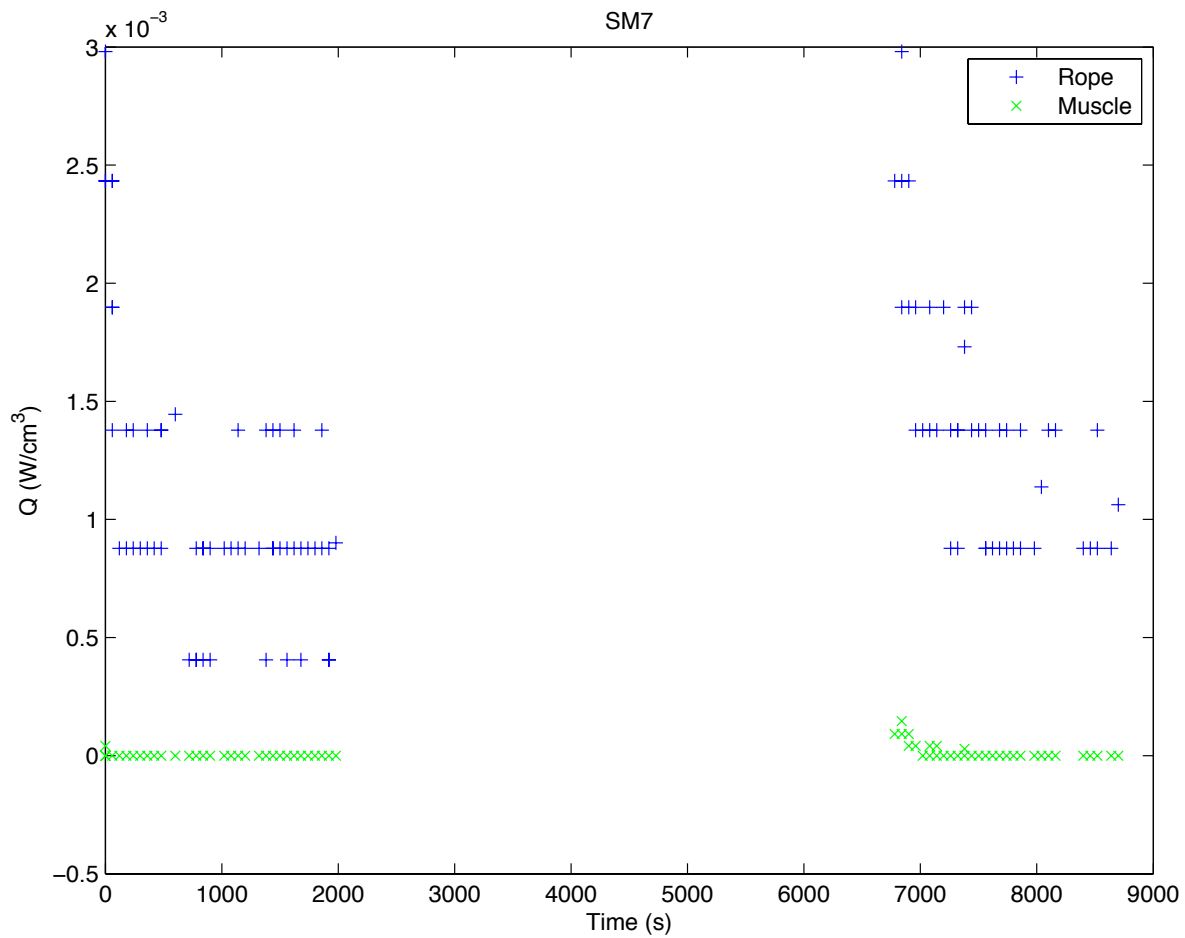


Figure 8: Heat generation in Lamprey 7

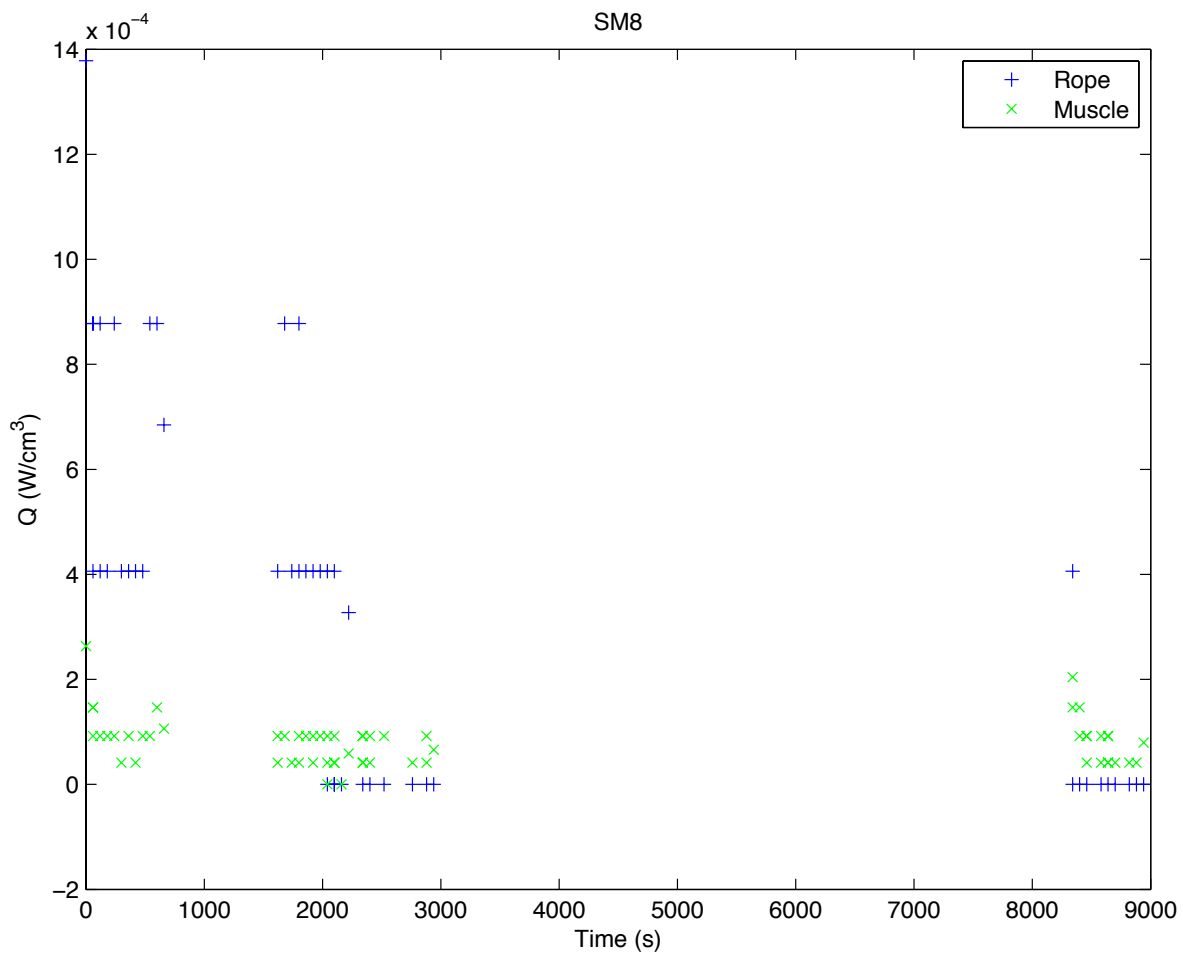


Figure 9: Heat generation in Lamprey 8

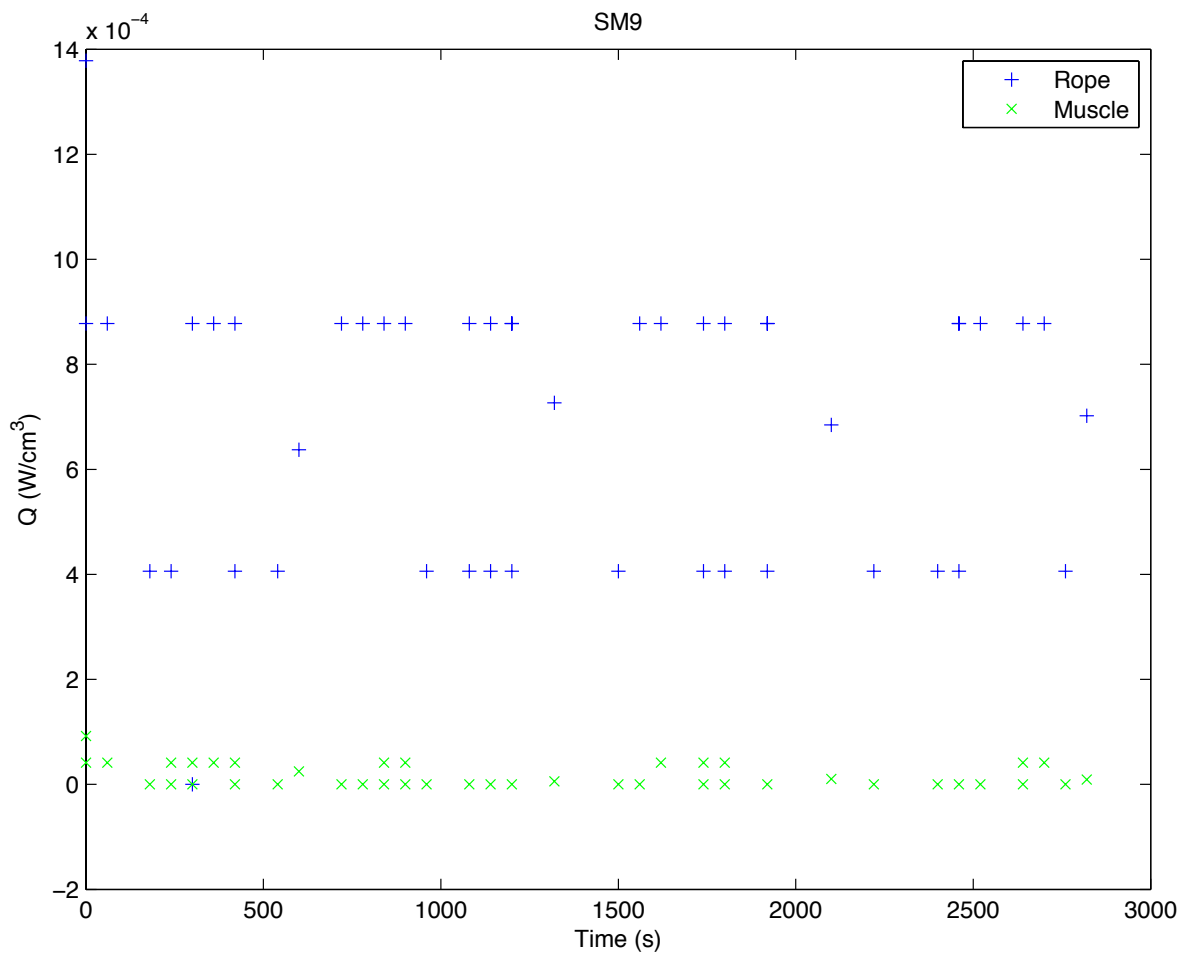


Figure 10: Heat generation in Lamprey 9

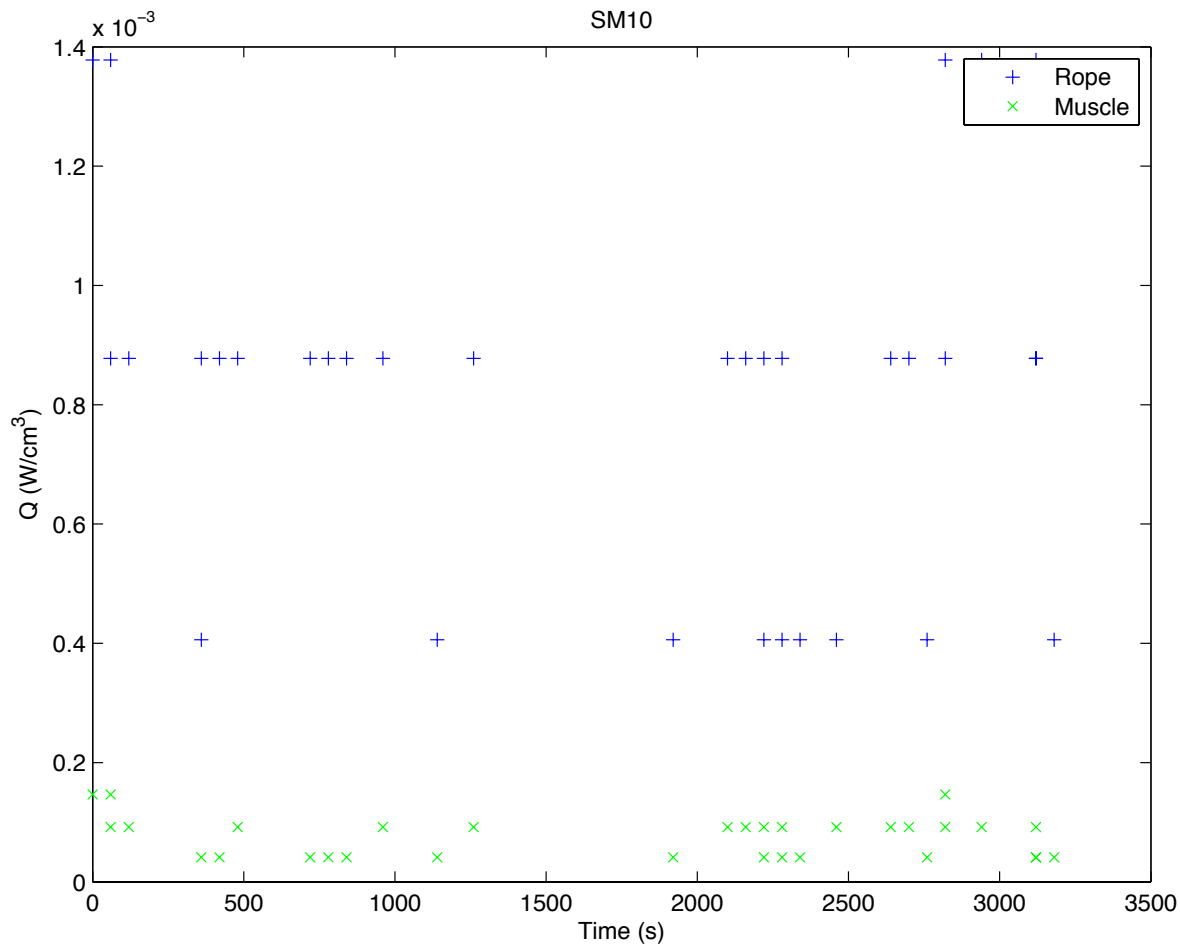


Figure 11: Heat generation in Lamprey 10

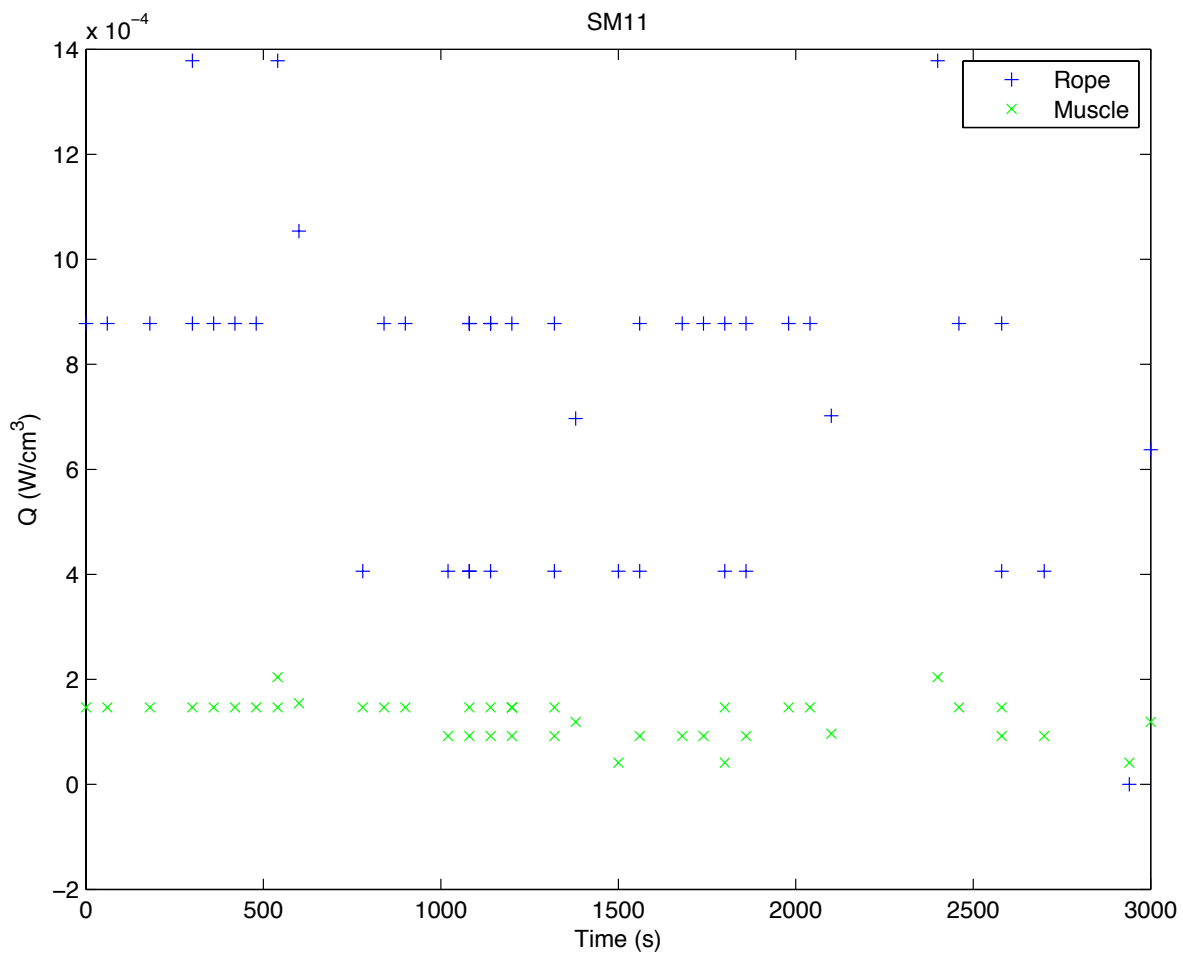


Figure 12: Heat generation in Lamprey 11

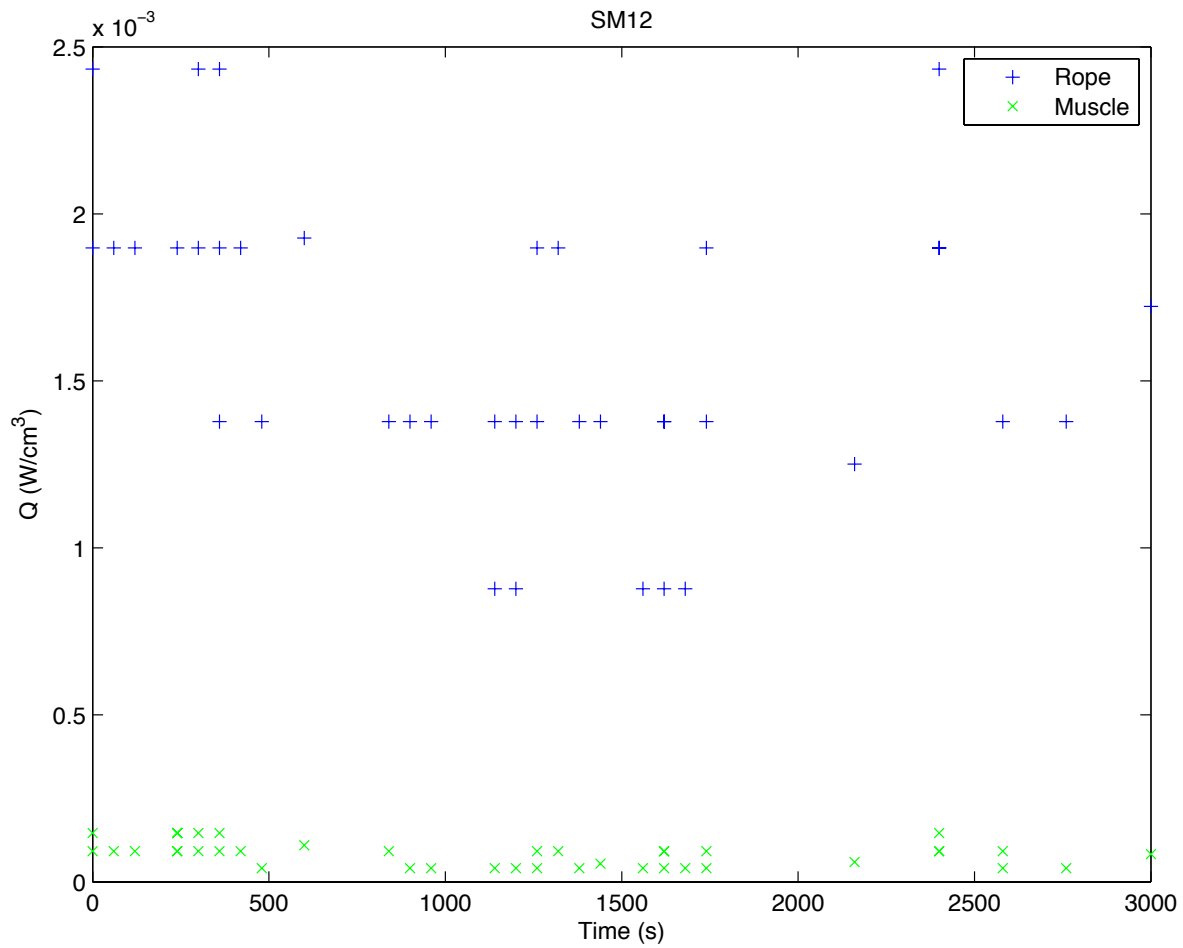


Figure 13: Heat generation in Lamprey 12

Bibliography

- [1] Incropera, F., and DeWitt, D., 2002. *Introduction to Heat Transfer, 4th edition.* John Wiley, New York.
- [2] Radhakrishnan, S., 1997. “Measurement of thermal properties of seafood”. Master’s thesis, Virginia Polytechnic Institute and State University.